Journal of the Mechanical Behavior of Biomedical Materials xxx (xxxx) xxx–xxx

Contents lists available at ScienceDirect

Journal of the Mechanical Behavior of Biomedical Materials

journal homepage: www.elsevier.com/locate/jmbbm

The mechanical importance of myelination in the central nervous system

Johannes Weickenmeier[a], Rijk de Rooij[a], Silvia Budday[b], Timothy C. Ovaert[c], Ellen Kuhl[d,*]

[a] Department of Mechanical Engineering, Stanford University, Stanford, CA 94305, USA
[b] Chair of Applied Mechanics, University of Erlangen-Nuremberg, 91058 Erlangen, Germany
[c] Department of Aerospace and Mechanical Engineering, The University of Notre Dame, Notre Dame, IN 46556, USA
[d] Departments of Mechanical Engineering and Bioengineering, Stanford University, Stanford, CA 94305, USA

ARTICLE INFO

Keywords:
Brain
Stiffness
Indentation
White matter
Myelin
Myelination

ABSTRACT

Neurons in the central nervous system are surrounded and cross-linked by myelin, a fatty white substance that wraps around axons to create an electrically insulating layer. The electrical function of myelin is widely recognized; yet, its mechanical importance remains underestimated. Here we combined nanoindentation testing and histological staining to correlate brain stiffness to the degree of myelination in immature, pre-natal brains and mature, post-natal brains. We found that both gray and white matter tissue stiffened significantly ($p \ll 0.001$) upon maturation: the gray matter stiffness doubled from 0.31 ± 0.20 kPa pre-natally to 0.68 ± 0.20 kPa post-natally; the white matter stiffness tripled from 0.45 ± 0.18 kPa pre-natally to 1.33 ± 0.64 kPa post-natally. At the same time, the white matter myelin content increased significantly ($p \ll 0.001$) from $58 \pm 2\%$ to $74 \pm 9\%$. White matter stiffness and myelin content were correlated with a Pearson correlation coefficient of $\rho = 0.92$ ($p \ll 0.001$). Our study suggests that myelin is not only important to ensure smooth electrical signal propagation in neurons, but also to protect neurons against physical forces and provide a strong microstructural network that stiffens the white matter tissue as a whole. Our results suggest that brain tissue stiffness could serve as a biomarker for multiple sclerosis and other forms of demyelinating disorders. Understanding how tissue maturation translates into changes in mechanical properties and knowing the precise brain stiffness at different stages of life has important medical implications in development, aging, and neurodegeneration.

1. Motivation

The white matter tissue of the healthy adult human brain contains more than 100,000 km of myelinated axons (Marner et al., 2003). Myelin, the membranous, lipid-rich sheath that wraps around axons, was discovered in 1854 (Virchow, 1854), and has since then been subject of extensive investigation. Myelin consists of 40% water and its dry mass is composed of 70-85% lipids and 15-30% protein (Morell and Quarles, 1999). Its high lipid content isolates the axon for efficient signal propagation and gives the tissue its characteristic white appearance.

The production of the myelin sheath is called myelination or myelinogenesis (Paus et al., 2001). Under the light microscope, we can visualize myelin using luxol fast blue straining (Kluver and Barrera, 1952), myelin basic protein staining, or glial fibrillary acidic protein staining (Urban et al., 1997). In humans, myelination begins during the third trimester of gestation, it increases progressively towards infancy, and continues throughout the first two decades of life (Budday et al., 2015). During myelination, oligodendrocytes, the myelinating cells of the central nervous system, selectively wrap axons with diameters larger than 0.2 μm Simons and Trajkovic, 2006. At the peak of myelination, oligodendrocytes can create up to three times their weight in membrane per day (McLaurin and Yong, 1995). While Schwann cells in the peripheral nervous system only myelinate a single axon, oligodendrocytes in the central nervous system can myelinate and cross-link up to 40 axons per oligodendrocyte (Baumann and Pham-Dinh, 2001). This results in a dense network of cross-linked cells as illustrated in Fig. 1. While it seems intuitive that this tightly cross-linked network affects the mechanical properties of the tissue, surprisingly, the neuron-oligodendrocyte network has not been acknowledged in any constitutive brain model to date.

The loss of the insulating myelin sheath is called demyelination and is a classical hallmark of some neurodegenerative or autoimmune diseases. One of the most common demyelinating diseases is multiple sclerosis (Streitberger et al., 2012), an unpredictable, often disabling disease of the central nervous system that affects 400,000 people in the

* Corresponding author.
E-mail address: ekuhl@stanford.edu (E. Kuhl).
URL: http://biomechanics.stanford.edu (E. Kuhl).

http://dx.doi.org/10.1016/j.jmbbm.2017.04.017
Received 8 April 2017; Accepted 12 April 2017

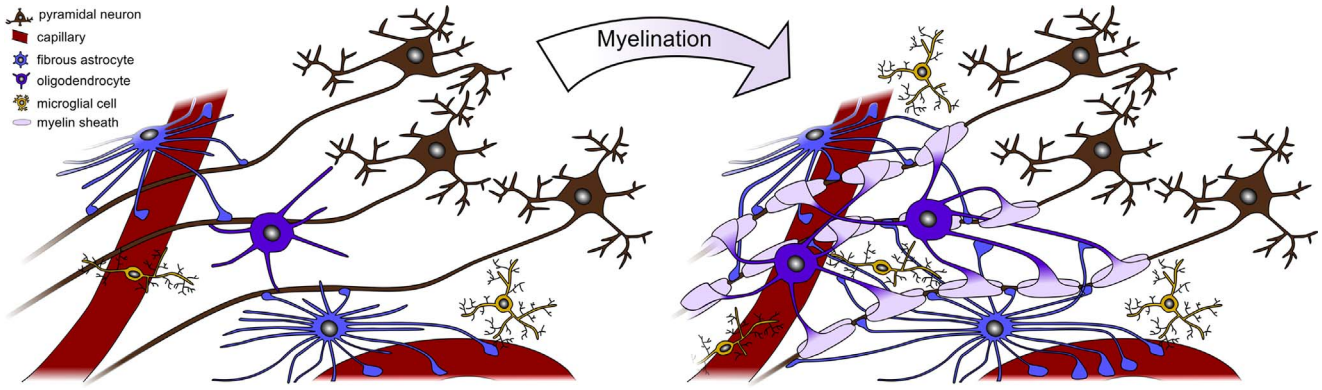

Fig. 1. Myelination in the white matter of the central nervous system. Oligodendrocytes, the myelinating cells of the central nervous system, wrap around axons and cross-link up to 40 axonal segments per oligodendrocyte. Fibrous astrocytes extend their processes to cross-link neurons, oligodendrocytes, other astrocytes, and endothelial cells around blood capillaries. Mechanically, myelination manifests itself in a dense network of tightly cross-linked cells that increases the mechanical stiffness. Histologically, myelination can be visualized using luxol fast blue staining.

United States alone, and more than 2 million worldwide (Zwibel and Smrtka, 2011). When myelin degrades, signal conduction is impaired or lost, and the nerve gradually withers. While the electrical effects of altered myelin concentrations are widely recognized, the mechanical effects of myelin remain poorly understood (Weickenmeier et al., 2016). Understanding the myelin changes in the developing brain and identifying their impact on brain mechanics is the objective of the present study.

2. Methods

To correlate brain stiffness to the degree of myelination, we combined mechanical characterization using nanoindentation (Zhang et al., 2010) and microstructural characterization using histological staining (Lejeune et al., 2016). We collected fresh pre-natal and post-natal bovine brains from a local slaughterhouse (Martin's Custom Butchering, Wakarusa, IN). Within two hours post mortem, we prepared 5-mm-thick sagittal slices from the center of the cerebral hemispheres using a customized cutting device.

Fig. 2 illustrates representative whole brains and sagittal slices. We placed each sagittal slice in a 100 mm-diameter petri dish and kept the samples refrigerated until testing. To slow down tissue degradation and prevent tissue dehydration, we hydrated the sample surfaces with phosphate-buffered saline solution (Budday et al., 2015). To minimize neurofilament protein alterations and ensure tissue integrity, we performed all tests within four hours post mortem (Weickenmeier et al., 2016).

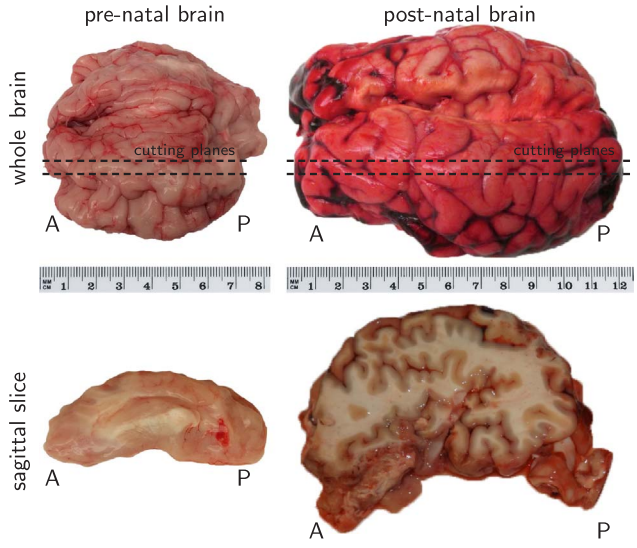

Fig. 2. Pre-natal and post-natal bovine brains for mechanical and microstructural characterization. We prepared 5-mm-thick sagittal slices to identify the white matter stiffness and the degree of myelination along the anterior-posterior arch of the corona radiata. A anterior, P posterior.

2.1. Mechanical characterization

To characterize the mechanical properties of the brain slices, we performed indentation testing on a Hysitron TI 950 TriboIndenter™ (Hysitron Inc., Eden Prairie, MN) equipped with an xZ 500 displacement stage (Budday et al., 2015). This setup extends the standard displacement range of the indenter tip to indentation depths of up to 500 μm with a 1 nm displacement control precision and a force measurement resolution of <0.1 nN. To ensure a homogeneous specimen response, we used a custom-made circular flat punch with a diameter of 1.5 mm (Blum and Ovaert, 2012, 2012). We performed all tests at room temperature and prescribed a trapezoidal loading-holding-unloading protocol towards a total indentation depth of 400 μm at a loading and unloading rate of 5 μm/s and a holding time of 10 s between loading and unloading (Budday et al., 2015). In this setup, the indentation force increases gradually during loading, decreases in response to stress relaxation during holding, and decreases gradually during unloading. Towards the end of unloading, the force becomes negative in response to tissue adhesion and returns to its initial value upon indenter-sample separation. To minimize adhesion between indenter and sample, we placed a 12 mm-diameter stainless steel washer around the testing site and added excess buffered saline solution to ensure a reproducible liquid film. We adopted a custom-designed algorithm to automatically detect the indenter-sample separation point and consistently zeroed forces and displacements across all measurements (Weickenmeier et al., 2016).

We interpreted the mean slope at 100 ± 10 μm of the loading curve as the contact stiffness k of each measurement. For this contact stiffness, we determined the effective elastic stiffness, $E_{\text{eff}} = \frac{1}{2}\, k\sqrt{\pi/A}$, where A is the projected contact area underneath the indenter (Oliver and Pharr, 2004). For our circular flat punch, the contact area $A = 1/4\pi d^2$ is independent of indentation depth and solely a function of punch diameter d and the effective elastic stiffness reduces to $E_{\text{eff}} = k/d$. The effective elastic stiffness accounts for the elastic deformation of the indenter with Young's modulus E_{ind} and Poisson's ratio ν_{ind} and of the sample with E_{smp} and ν_{smp}, and takes the following form $1/E^{\text{eff}} = (1-\nu_{\text{ind}}^2)/E_{\text{ind}} + (1-\nu_{\text{smp}}^2)/E_{\text{smp}}$ (Oliver and Pharr, 2004). For brain tissue, the indenter stiffness is orders of magnitudes larger than the sample stiffness, $E_{\text{ind}} \gg E_{\text{smp}}$, and we can approximate the elastic modulus of the sample by $E_{\text{smp}} = (1-\nu_{\text{smp}}^2)E_{\text{eff}}$. With the common assumption of incompressibility, $\nu_{\text{smp}} = 0.5$, the sample stiffness simplifies to $E_{\text{smp}} = \frac{3}{4}\, k/d$. We tested eleven brain samples of pre- and

postnatal bovine brains and performed a total of $n=130$ indentation tests, $n=11$ in the pre-natal gray matter, $n=18$ in the post-natal gray matter, $n=21$ in the pre-natal white matter, and $n=80$ in the post-natal white matter.

2.2. Histological characterization

Following mechanical testing we prepared the indented samples for light microscopy. We fixed the samples using 10% buffered formalin of 4% formaldehyde in phosphate buffered saline solution, gradually dehydrated the samples by replacing tissue water by alcohol, cleared the samples by replacing alcohol by xylene, and embedded the dehydrated samples in paraffin wax blocks. From these, we prepared 8-10 nm thick histological slices using a microtome.

We stained the histological slices using hematoxylin and eosin (H & E), luxol fast blue (LFB), myelin based protein (MBP), and glial fibrillary acidic protein (GFAP). Hematoxylin and eosin (H & E) staining consists of a hematoxylin stain that colors cell nuclei in blue and a subsequent eosin counterstain that colors eosinophilic intracellular and extracellular protein structures in shades of red, pink, and orange. Luxol fast blue (LFB) staining colors myelin in blue, neuropil in pink, and nerve cells in purple. Myelin based protein (MBP) immunohistochemistry uses antibodies that recognize myelin basic protein, a major constituent of the myelin sheath of oligodendrocytes of the central nervous system. Glial fibrillary acidic protein (GFAP) staining highlights intermediate filament proteins expressed by numerous cell types of the central nervous system including astrocytes. The combined hematoxylin and eosin and luxol fast blue stain (H & E-LFB) allows us to characterize the myelin content in white matter tissue. Using image analysis tools of MATLAB, we differentiated the stain into red and purple (H & E) to highlight the neuroglial network and blue (LFB) to highlight myelin. We quantified the relative area fraction of the red- and blue-colored regions, and interpreted the blue-colored area fraction as the local myelin content (Weickenmeier et al., 2016).

3. Results

3.1. Mechanical characterization

Fig. 3 summarizes the results of our $n=130$ indentation tests. Overall, our average white matter stiffness of 1.15 ± 0.68 kPa was more than twice as large as the average gray matter stiffness of 0.54 ± 0.27 kPa. In the gray matter tissue, the pre-natal stiffness of 0.31 ± 0.20 kPa was significantly lower ($p < 10^{-4}$) than the average post-natal stiffness of 0.68 ± 0.20 kPa. Similarly, in the white matter tissue, the average pre-natal stiffness of 0.45 ± 0.18 kPa was significantly lower ($p < 10^{-8}$) than the average post-natal stiffness of

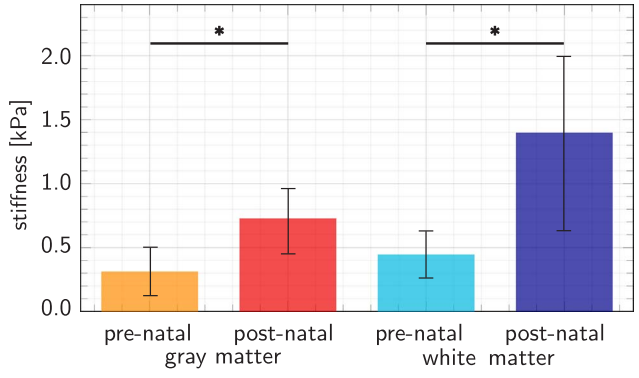

Fig. 3. In a total of $n=130$ indentation tests, the pre-natal gray and white matter stiffnesses of 0.31 ± 0.20 kPa and 0.45 ± 0.18 kPa were significantly smaller than the post-natal gray ($p < 10^{-4}$) and white ($p < 10^{-8}$) matter stiffnesses of 0.68 ± 0.2 kPa and 1.33 ± 0.64 kPa.

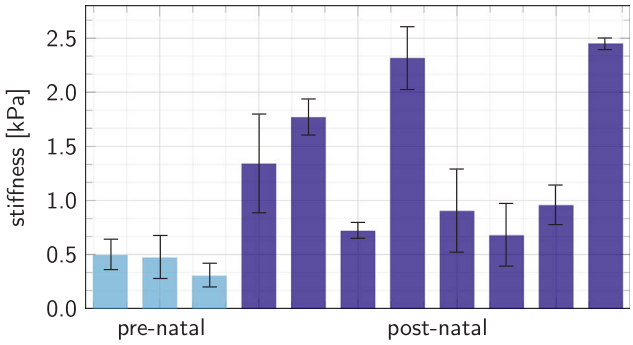

Fig. 4. In a total of $n=11$ samples, the pre-natal white matter stiffness varied between 0.15 kPa and 0.79 kPa whereas the post-natal white matter stiffness varied between 0.34 kPa and 2.93 kPa. Inter-sample variations in white matter stiffness were larger than intra-sample variations.

1.33 ± 0.64 kPa. The average stiffness ratio between white and gray matter increased from 1.5 in the immature pre-natal brain to 2.0 in the mature post-natal brain. Of all tissue regions, the mature post-natal white matter tissue displayed the largest overall variation. To explore whether this variation was sample specific, we analyzed the white matter stiffnesses of the individual samples.

Fig. 4 summarizes the white matter stiffnesses of $n=11$ samples, with n = 3 from immature, pre-natal tissue and n = 8 from mature, post-natal tissue, each covering three to six indentation sites. The recorded pre-natal white matter stifnesses varied between 0.15 kPa and 0.79 kPa, whereas the post-natal white matter stiffnesses varied between 0.34 kPa and 2.93 kPa. The average stiffness of all three pre-natal samples was lower than the average stiffness of any of the eight post-natal samples. While the pre-natal stiffnesses were relatively homogeneous across all samples, the post-natal stiffnesses displayed large stiffness variations. Fig. 4 reveals that variations in white matter stiffness result primarily from inter-sample variations rather than from intra-sample variations.

3.2. Histological characterization

Fig. 5 illustrates the histological stains of cerebral and cerebellar

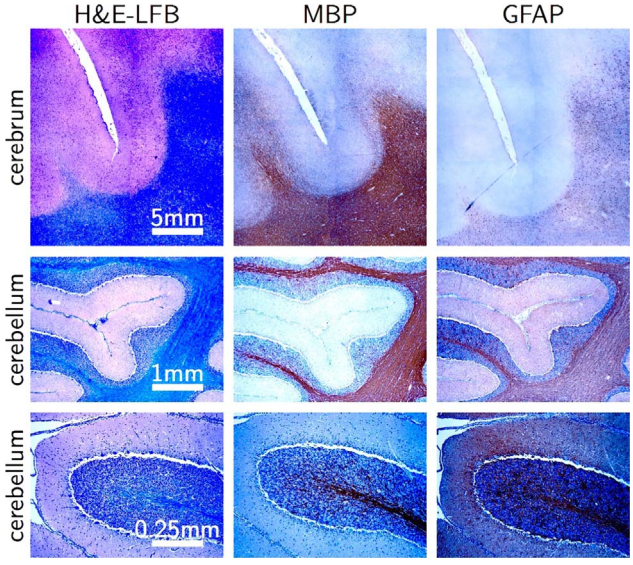

Fig. 5. Histological characterization of cerebral and cerebellar white and gray matter. The hematoxylin and eosin and luxol fast blue (H & E-LFB) stain, the myelin basic protein (MBP) stain, and the glial fibrillary acidic protein (GFAP) stain highlight myelinated axons in the white matter in blue and brown. The hematoxylin and eosin and luxol fast blue (H & E-LFB) stain additionally visualizes neuronal cell bodies and cell processes in the gray matter in purple. (For interpretation of the references to color in this figure legend, the reader is referred to the web version of this article.)

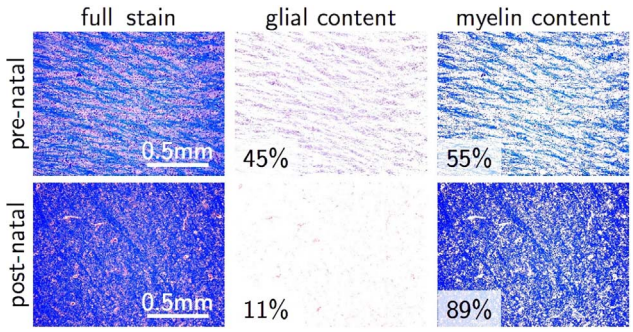

Fig. 6. Representative hematoxylin and eosin and luxol fast blue (H & E-LFB) stains of pre-natal and post-natal cerebral white matter tissue. Image processing differentiates between glial and myelin contents based on color separation. Samples illustrate lower and upper limits of myelin content across all $n = 11$ samples. The image width corresponds to the indenter diameter of 1.5 mm. (For interpretation of the references to color in this figure legend, the reader is referred to the web version of this article.)

white and gray matter tissue. The first row shows the interface between cerebral gray and white matter in a sulcus. The second row shows the cortical and subcortical interface in the cerebellum. The third row shows a magnification of a cerebellar gyrus with its distinct three-layered morphology with the superficial molecular layer, the layer of Purkinje cells, and the inner granular layer. The hematoxylin and eosin and luxol fast blue (H & E-LFB) stain highlights myelinated axons in the white matter tissue in blue and neuronal cell bodies and cell processes in the gray matter tissue in purple. This creates a distinct color separation between the cortical and subcortical layers. The myelin basic protein (MBP) stain illustrates myelin in brown and highlights the dense myelin network in the white matter tissue. At the same time, it illustrates the penetration of individual axons into the cortical gray matter tissue. The glial fibrillary acidic protein (GFAP) stain visualizes glial cells and highlights the dense network of astrocytes within the white matter tissue. At increased magnification, this stain highlights the underlying glial scaffold for neurons in the gray matter and axons in the white matter tissue.

Fig. 6 shows representative hematoxylin and eosin and luxol fast blue (H & E-LFB) stains of pre-natal and post-natal cerebral white matter tissue. The image dimensions corresponds approximately to the indenter diameter of 1.5 mm. The full stain can be processed via color separation to differentiate between glial and myelin content. In the histochemical analysis of the $n = 11$ samples, we observed a variation in the myelin content ranging from as low as 55% in the pre-natal brain to 89% in the post-natal brains.

Fig. 7 summarizes the relationship between the cerebral white matter stiffness and the local myelin content for the $n = 11$ samples. The light blue and dark blue dots indicate the mean stiffness and myelin content of the pre- and post-natal brains determined from the image analysis of the luxol fast blue stains. The ellipses visualize the standard deviations in stiffness and myelin content. The average myelin content of the pre-natal samples of 58 ± 2% was significantly lower ($p < 10^{-5}$) than the average myelin content of the post-natal samples of 74 ± 9%. The white matter tissue stiffens with increasing myelin content with a Pearson correlation coefficient of $\rho = 0.92$ ($p < 10^{-4}$). When determining the myelin content from the myelin basic protein stain illustrated in the second column of Fig. 5, rather than from the luxol fast blue stain illustrated in the first column, the correlation between white matter tissue stiffness and myelin content was slightly less pronounced with a Pearson correlation coefficient of $\rho = 0.59$ ($p < 0.05$).

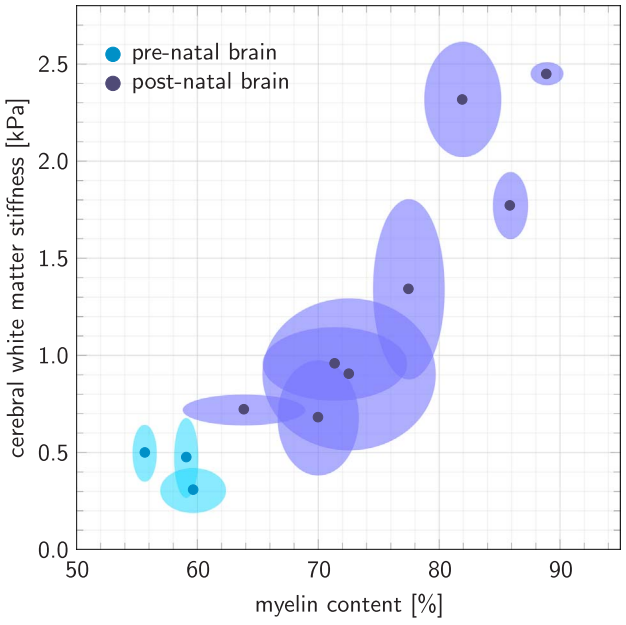

Fig. 7. Stiffness-myelin relation in different regions of cerebral white matter. The average myelin content of the pre-natal samples of 58 ± 2% was significantly lower ($p < 10^{-5}$) than the average myelin content of the post-natal samples of 74 ± 9%. Across all $n = 11$ samples, the stiffness increased with increasing myelin content with a Pearson correlation coefficient of $\rho = 0.92$ ($p < 10^{-4}$). Dots indicate mean, ellipses indicate standard deviations in stiffness and myelin content. (For interpretation of the references to color in this figure legend, the reader is referred to the web version of this article.)

4. Discussion

4.1. Variations between gray and white matter

The current literature provides a wide range of brain tissue stiffnesses with different and often contradicting gray to white matter stiffness ratios (Budday et al., 2015, 2017; Christ et al., 2010; Pervin and Chen, 2009). Testing methods, loading conditions, and sample morphology have a significant impact on the reported mechanical properties (Budday et al., 2017; Chatelin et al., 2017; Franceschini et al., 2006; Franze et al., 2013; Mihai et al., 2015; Prevost et al., 2011; Rashid et al., 2012, 2014). Stiffness discrepancies–especially within one and the same brain, tested under the same loading conditions–have recently motivated the study of regional microstructural variations to rationalize the observed differences (Weickenmeier et al., 2016).

In this study, in Fig. 3, white matter was stiffer than gray matter. On average, our measured white matter stiffness with 1.15 ± 0.68 kPa was more than twice as stiff as our gray matter stiffness with 0.54 ± 0.27 kPa. These stiffness differences agree well with previous indentation tests (Budday et al., 2015; Weickenmeier et al., 2016), but contradict tests of isolated tissue samples in tension, compression, and shear (Budday et al., 2017). We hypothesize that these differences between intact tissue slices and isolated tissue samples can be attributed–at least in part–to the pore fluid within the tissue (Franceschini et al., 2006), which can easily escape the isolated samples, but not the intact slices studied here. Gray and white matter tissue have different permeabilities and different fluid volume fractions (Whittall et al., 1997), which could explain these discrepancies.

In addition to different permeabilities and volume fractions, our histological stains in Fig. 5 reveal marked differences in tissue microstructure between gray and white matter. It is well-known that the mechanical properties of biological tissues are highly sensitive to the underlying microstructural architecture (Meyers et al., 2008), and that many biological systems use this sensitivity as guiding principle for optimal design (Meyers et al., 2013). In the brain, gray matter consists primarily of neuronal cell bodies and a dense network of dendritic connections, whereas white matter consists of long myelinated axons that are embedded in a tightly connected network of neuroglial cells, and oligodendrocytes (Goriely et al., 2015). These microstructural differences could explain stiffness differences between gray and white matter as highlighted in Fig. 3.

4.2. Variations between pre- and post-natal tissue

The objective of the present study was to investigate mechanical stiffness variations in response to tissue maturation. From a biochemical perspective, it is broadly accepted that brain tissue undergoes significant changes throughout life (Baumann and Pham-Dinh, 2001; Urban et al., 1997). Yet, precisely how tissue maturation translates into changes in mechanical properties remains insufficiently understood. Our results in Figs. 3 suggest that both gray and white matter tissue stiffen upon maturation. Specifically, gray matter stiffness doubled from 0.31 ± 0.20 kPa pre-natally to 0.68 ± 0.20 kPa post-natally, while the white matter stiffness even tripled from 0.45 ± 0.18 kPa pre-natally to 1.33 ± 0.64 kPa post-natally.

Notably, with measurements from 0.15 kPa to 2.93 kPa, our white matter stiffnesses in Fig. 4 varied by more than one order of magnitude. In the immature pre-natal brain, white matter stiffnesses varied by 40% compared to 52% in the mature post natal brain. These variations can potentially be explained by a temporal variation in myelin deposition in the developing brain (Schindler et al., 1990) and a regional variation in myelin content in the mature brain (Weickenmeier et al., 2016). To further elaborate this explanation, we quantified the local myelin content. Fig. 5 summarizes our three different stains to quantify the degree of myelination, luxol fast blue, myelin basic protein, and glial fibrillary acidic protein stains. Of these, the luxol fast blue stain revealed variations in myelin content between 55% and 89%. The local myelin content increased from $58 \pm 2\%$ pre-natally to $74 \pm 9\%$ post-natally. When correlating variations in white matter stiffness to myelin content in Fig. 7, we observed a Pearson correlation coefficient of $\rho = 0.92$. For comparison, we also calculated the Pearson correlation coefficient for the myelin basic protein stain of $\rho = 0.59$ and concluded that, for this study, the luxol fast blue strain would be most appropriate (Urban et al., 1997). Our trend of tissue stiffening with increasing myelin agrees with our previous observations in mature brains (Weickenmeier et al., 2016) where we found a Pearson correlation coefficient of $\rho = 0.91$. These findings suggest that spatial and temporal variations in myelin content have a significant impact on the brain's mechanical properties (Paus, 2010).

Fig. 1 illustrates the different cell types that will contribute to the overall mechanical response of white matter tissue: Neurons, astrocytes, oligodendrocytes, and microglia. Taken together, these cells provide a dense structural scaffold with an inherent mechanical stiffness that is yet unknown. Our luxol fast blue stains in Figs. 5 and 6 only quantify the degree of myelination as an indicator for the dense network of oligodendrocytes. While our study reveals that oligodendrocytes are an important contributor to the load-bearing cellular microstructure (Baumann and Pham-Dinh, 2001), other cell types and the extracellular matrix could have similar effects that we have not addressed here.

Much in contrast to the human brain, where myelination accelerates after birth and continues throughout the first two decades in life in response to the development of motor control, speech, and cognitive skills (Budday et al., 2015), myelination in the bovine brain is almost fully completed at the time of birth (Urban et al., 1997). This might explain the noticeable myelin content of $58 \pm 2\%$ in our pre-natal brain samples. Similar to sheep brain (Barlow, 1969), myelination in the bovine brain occurs rapidly during the third trimester of gestation and is almost completed upon birth (Urban et al., 1997).

4.3. Clinical implications

In humans, myelination takes place mainly after birth and continues throughout the first two decades of life (Paus, 2010). Knowing the precise brain stiffness at different stages of life is critical to interpret and potentially modulate biochemical and mechanical cues during neuronal development (Koser et al., 2016), oligodendrocyte differentiation (Lourenco et al., 2016), and maturation. Incomplete myelination at birth could help explain why immature brains are softer than mature, fully myelinated brains and more vulnerable to mechanical insult. An important clinical and legal implication of stiffness changes upon myelination is shaken baby syndrome (Goriely et al., 2015): During maturation, myelination, associated with an increase in stiffness, could partially explain the discrepancies between the injury thresholds established for adults and the much lower critical injury levels observed in babies (Duhaime et al., 1987). Conversely, during aging, the marked loss of myelinated axons, at a rate of 10% per decade (Marner et al., 2003), could explain the observed stiffness decline of 0.8% per year (Sack et al., 2009). Similarly, a recent study in rats reported a significant loss in white matter stiffness in response to controlled injury, both in the spinal cord and in the central nervous system (Moeendarbary et al., 2017). Comprised white matter integrity has also been associated with a high risk of psychosis, and a decreased number of oligodendrocytes has been reported in schizophrenia patients (Chew et al., 2013).

With a view towards demyelinating disorders, understanding the interplay between myelination and tissue stiffness has important clinical implications: Rapid developments in magnetic resonance elastography now allows us to directly visualize and quantitatively measure brain tissue stiffnesses in vivo (Feng et al., 2013; Kruse et al., 2008). Recent studies suggest that neuro-inflammatory diseases associated with the demyelination of white matter axons lead to a reduction in brain elasticity (Schregel et al., 2012). Magnetic resonance elastography confirmed a close correlation between demyelination in chronic-progressive multiple sclerosis and a decrease in brain tissue stiffness (Streitberger et al., 2012). Similarly, reduced brain tissue stiffnesses were observed in patients with Alzheimer's disease (Murphy et al., 2011). This suggests that tissue stiffness could serve as an in vivo biomarker for neurodegeneration (van den Bedem and Kuhl, 2017).

4.4. Limitations

Our presented study is limited by a few aspects that could benefit from further investigation. First, by the design of the study, our analysis is based on bovine brain samples, not human. Although the gestation period of nine months is similar in cows and humans, myelination of bovine brains is almost complete at birth, while it continues throughout the first two decades of life in humans. However, since our major result is a structure-function relationship between stiffness and myelin content, our findings are independent of species and age. Yet, in the future, it would be interesting to correlate stiffness, myelination, and age in humans. Second, while our study is limited by the small sample size, our findings were statistically significant: Our pre-natal samples were significantly softer than our post-natal samples and displayed a markedly lower myelin content. It would be interesting to expand the study towards more pre-natal samples with the goal to characterize the time line of stiffening and, with it, the stiffness of completely unmyelinated brains. Third, our testing method inherently probes brain tissue samples ex vivo and is incapable of quantifying in vivo effects. Magnetic resonance elastography could provide further insight into brain tissue stiffnesses in vivo, especially when directly compared and calibrated with ex vivo measurements.

5. Concluding remarks

Motivated by large inter-specimen variations in tissue stiffness, we have correlated white matter stiffness to the degree of myelination in pre-natal and post-natal brains. We showed that white matter stiffness increases with increasing myelination and that immature, pre-natal tissue is both, less stiff and less myelinated, than mature, post-natal tissue. Our study suggests that myelin is not only important to ensure smooth electrical signal propagation in neurons, but also to protect neurons against physical forces and provide a strong microstructural network that stiffens the white matter tissue as a whole. From a basic science point of view, our findings can inform microstructurally-

motivated constitutive models and serve as validation tool for magnetic-resonance-image based in vivo stiffness measurements of the brain. From a clinical point of view, our results suggest that brain tissue stiffness could serve as a biomarker for multiple sclerosis and other forms of demyelinating disorders.

Acknowledgements

We acknowledge the stimulating discussions and support of Hannes Vogel. This work was supported by the German National Science Foundation grant STE 544/50-1 to Silvia Budday, by the Stanford Graduate Fellowship to Rijk de Rooij, and by a Stanford Bio-X Interdisciplinary Initiatives Seed Grant to Johannes Weickenmeier and Ellen Kuhl.

References

Barlow, R.M., 1969. The fetal sheep: morphogenesis of the nervous system and histochemical aspects of myelination. J. Comp. Neurol. 135, 249–261.
Baumann, N., Pham-Dinh, D., 2001. Biology of oligodendrocyte and myelin in the mammalian central nervous system. Physiol. Rev. 81, 871–927.
Blum, M.M., Ovaert, T.C., 2012. Experimental and numerical tribological studies of a boundary lubricant functionalized poro-viscoelastic PVA hydrogel in normal contact and sliding. J. Mech. Behav. Biomed. Mater. 14, 248–258.
Blum, M.M., Ovaert, T.C., 2012. A novel polyvinyl alcohol hydrogel functionalized with organic boundary lubricant for use as low-friction cartilage substitute: Synthesis, physical/chemical, mechanical, and friction characterization. J. Biomed. Mater. Res. B: Appl. Biomater. 100, 1755–1763.
Budday, S., Steinmann, P., Kuhl, E., 2015. Physical biology of human brain development. Front. Cell. Neurosci. 9, 257.
Budday, S., Nay, R., de Rooij, R., Steinmann, S., Wyrobek, T., Ovaert, C.T., Kuhl, E., 2015. Mechanical properties of gray and white matter brain tissue by indentation. J. Mech. Behav. Biomed. Mater. 46, 318–330.
Budday, S., Sommer, G., Birkl, C., Langkammer, C., Hayback, J., Kohnert, J., Bauer, M., Paulsen, F., Steinmann, P., Kuhl, E., Holzapfel, G.A., 2017. Mechanical characterization of human brain tissue. Acta Biomater. 48, 319–340.
Budday, S., Sommer, G., Steinmann, P., Kuhl, E., Holzapfel, G.A., 2017. Rheological Characterization of Human Brain Tissue. submitted for publication.
Chatelin, S., Constantinesco, A., Willinger, R., 2017. Fifty years of brain tissue mechanical testing: from in vitro to in vivo investigations. Biorheology 47, 255–276.
Chew, L.J., Fusar-Poli, P., Schmitz, T., 2013. Oligodendrocyte alterations and the role of microglia in white matter injury: Relevance to schizophrenia. Dev. Neurosci. 35, 102–129.
Christ, A.F., Franze, K., Gautier, H., Moshayedi, P., Fawcett, J., Franklin, R.J.M., Karadottir, R.T., Guck, J., 2010. Mechanical difference between white and gray matter in the rat cerebellum measured by scanning force microscopy. J. Biomech. 43, 2986–2992.
Duhaime, A.C., Gennarelli, T.A., Thibault, L.E., Bruce, D.A., Margulies, S.S., Wiser, R., 1987. The shaken baby syndrome. J. Neurosurg. 66, 409–415.
Feng, Y., Clayton, E.H., Chang, Y., Okamoto, R.J., Bayly, P.V., 2013. Viscoelastic properties of the ferret brain measured in vivo at multiple frequencies by magnetic resonance elastography. J. Biomech. 46, 863–870.
Franceschini, G., Bigoni, D., Regitnig, P., Holzapfel, G.A., 2006. Brain tissue deforms similar to filled elastomers and follows consolidation theory. J. Mech. Phys. Solids 54, 2592–2620.
Franze, K., Janmey, P.A., Guck, J., 2013. Mechanics in neuronal development and repair. Ann. Rev. Biomed. Eng. 15, 227–251.
Goriely, A., Budday, S., Kuhl, E., 2015. Neuromechanics: from neurons to brain. Adv. Appl. Mech. 48, 79–139.
Goriely, A., Geers, M.G.D., Holzapfel, G.A., Jayamohan, J., Jerusalem, A., Sivaloganathan, S., Squier, W., van Dommelen, J.A.W., Waters, S., Kuhl, E., 2015. Mechanics of the brain: Perspectives, challenges, and opportunities. Biomech. Model. Mechanobiol. 14, 931–965.
Kluver, H., Barrera, E.A., 1952. A method for the combined staining of cells and fibers in the nervous system. J. Neuropathol. Exp. Neurol. 12, 400–403.
Koser, D.E., Thompson, A.J., Foster, S.K., Dwivedy, A., Pillai, E.K., Sheridan, G.K., Svoboda, H., Viana, M., Costa, L.d.F., Guck, J., Holt, C.E., Franze, C., 2016. Mechanosensing is critical for axon growth in the developing brain. Nat. Neurosci. 19, 1592–1598.
Kruse, S.A., Rose, G.H., Glaser, K.J., Manduca, A., Felmlee, J.P., Jack, C.R., Ehman, R.L., 2008. Magnetic resonance elastography of the brain. Neuroimage 39, 231–237.
Lejeune, E., Javili, A., Weickenmeier, J., Kuhl, E., Linder, C., 2016. Tri-layer wrinkling as a mechanism for anchoring center initiation in the developing cerebellum. Soft Matter 12, 5613–5620.
Lourenco, T., de Faria, J.P., Bippes, C.A., Maia, J., Lopes-da-Silva, J.A., Relvas, J.B., Graos, M., 2016. Modulation of oligodendrocyte differentiation and maturation by combined biochemical and mechanical cues. Sci. Rep. 6, 21563.
Marner, L., Nyengaard, J.R., Tang, Y., Pakkenberg, B., 2003. Marked loss of myelinated nerve fibers in the human brain with age. J. Comp. Neurol. 462, 144–152.
McLaurin, J.A., Yong, V.W., 1995. Oligodendrocytes and myelin. Neurol. Clin. 13, 23–49.
Meyers, M.A., Chen, P.Y., Lin, A.Y.M., Seki, Y., 2008. Biological materials: structure and mechanical properties. Prog. Mater. Sci. 53, 1–206.
Meyers, M.A., McKittrick, J., Chen, P.Y., 2013. Structural biological materials: critical mechanics-material connections. Science 339, 773–779.
Mihai, L.A., Chin, L.K., Janmey, P.A., Goriely, A., 2015. A comparison of hyperelastic constitutive models applicable to brain and fat tissues. J. Roy. Soc. Int. 12, 20150486.
Moeendarbary, E., Weber, I.P., Sheridan, G.K., Koser, D.E., Soleman, S., Haenzi, B., Bradbury, E.J., Fawcell, J., Franze, K., 2017. The soft mechanical signature of glial scars in the central nervous system. Nat. Comm. 8, 14787.
Morell, P., Quarles, R.H., 1999. Characteristic composition of myelin. In: Siegel, G.J., Agranoff, B.W., Albers, R.W., Fisher, S.K., Uhler, M.D. (Eds.), Basic Neurochemistry: Molecular, Cellular and Medical Aspects, 6th edition. Lippincott-Raven, Philadelphia.
Murphy, M.C., Huston, J., Jack, C.R., Glaser, K.J., Manduca, A., Felmlee, J.P., Ehman, R.L., 2011. Decreased brain stiffness in Alzheimer's disease determined by magnetic resonance elastography. J Magn. Reson. Imaging 34, 494–498.
Oliver, W.C., Pharr, G.M., 2004. Measurement of hardness and elastic modulus by instrumented indentation: advances in understanding and refinements to methodology. J. Mater. Res. 19, 3–20.
Paus, T., Collins, D.L., Evans, A.C., Leonard, G., Pike, B., Zijdenbos, A., 2001. Maturation of white matter in the human brain: a review of magnetic resonance studies. Brain Res. Bull. 54, 255–266.
Paus, T., 2010. Growth of white matter in the adolescent brain: myelin or axon? Brain Cogn. 72, 26–35.
Pervin, F., Chen, W.W., 2009. Dynamic mechanical response of bovine gray matter and white matter brain tissues under compression. J. Biomech. 42, 731–735.
Prevost, T.P., Balakrishnan, A., Suresh, S., Socrate, S., 2011. Biomechanics of brain tissue. Acta Biomater. 7, 83–95.
Rashid, B., Destrade, M., Gilchrist, M.D., 2012. Determination of friction coefficient in unconfined compression of brain tissue. J. Mech. Behav. Biomed. Mater. 14, 163–171.
Rashid, B., Destrade, M., Gilchrist, M.D., 2014. Mechanical characterization of brain tissue in tension at dynamic strain rates. J. Mech. Behav. Biomed. Mater. 33, 43–54.
Sack, I., Beierback, B., Wuerfel, J., Klatt, D., Hamhaber, U., Papazoglou, S., Martus, P., Braun, J., 2009. The impact of aging and gender on brain viscoelasticity. NeuroImage 46, 652–657.
Schindler, P., Luu, B., Sorokine, O., Trifilieff, E., Van Dorsselaer, A., 1990. Developmental study of proteolipids in bovine brain: A novel proteolipid and dm-20 appear before proteolipid protein (plp) during myelination. J. Neurochem. 55, 2079–2085.
Schregel, K., Wuerfel, E., Garteiser, P., Gemeinhardt, I., Prozorovski, T., Aktas, O., Merz, H., Petersen, D., Wuerfel, J., Sinkus, R., 2012. Demyelination reduces brain parenchymal stiffness quantified in vivo by magnetic resonance elastography. Proc. Nat. Acad. Sci. 109, 6650–6655.
Simons, M., Trajkovic, K., 2006. Neuron-glia communication in the control of oligodendrocyte function and myelin biogenesis. J. Cell Sci. 119, 4381–4389.
Streitberger, K.J., Sack, I., Krefting, D., Pfüller, C., Braun, J., Paul, F., Wuerfel, J., 2012. Brain viscoelasticity alteration in chronic-progressive multiple sclerosis. PloS One 7, e29888.
Urban, K., Hewicker-Trautwein, M., Trautwein, G., 1997. Development of myelination in the bovine fetal brain: an immunohistochemical study. Anat. Histol. Embryol. 26, 187–192.
van den Bedem, H., Kuhl, E., 2017. Molecular mechanisms of chronic traumatic encephalopathy. Curr. Opionion Biomed. Eng.. http://dx.doi.org/10.1016/j.cobme.2017.02.003. (online first).
Virchow, R., 1854. Ueber das ausgebreitete Vorkommen einer dem Nervenmark analogen Substanz in den thierischen Geweben. Virchows Arch. 6, 562–572.
Weickenmeier, J., de Rooij, R., Budday, S., Steinmann, P., Ovaert, T.C., Kuhl, E., 2016. Brain stiffness increases with myelin content. Acta Biomater. 42, 265–272.
Whittall, K., Mackay, A.L., Graeb, D.A., Nugent, R.A., Li, D.K.B., Paty, D.W., 1997. In vivo measurements of T_2 distributions and water content in normal human brain. Magn. Res. Med. 37, 34–43.
Zhang, J., Michalenko, M.M., Kuhl, E., Ovaert, T.C., 2010. Characterization of indentation response and stiffness reduction of bone using a continuum damage model. J. Mech. Behav. Biomed. Mater. 3, 189–202.
Zwibel, H.L., Smrtka, J., 2011. Improving quality of life in multiple sclerosis: An unmet need. Am. J. Manag. Care 17, S139–S145.